JP1.6

AN OBJECTIVE EVALUATION AND REGIME CLASSIFICATION OF RAMS FORECAST ERRORS DURING THE 2000 FLORIDA WARM SEASON

Jonathan L. Case*, John Manobianco, and Allan V. Dianic
NASA Kennedy Space Center / Applied Meteorology Unit / ENSCO, Inc.

Dewey E. Harms
45th Weather Squadron, United States Air Force, Patrick AFB, FL

Paul N. Rosati
45th Space Wing, Eastern Range Safety, United States Air Force, Patrick AFB, FL

1. INTRODUCTION

This paper presents a portion of the Applied Meteorology Unit's (AMU) evaluation of the Regional Atmospheric Modeling System (RAMS) contained within the Eastern Range Dispersion Assessment System (ERDAS). ERDAS is designed to provide emergency response guidance for operations at the Cape Canaveral Air Force Station (CCAFS) and Kennedy Space Center (KSC), Florida, in the event of an accidental hazardous material release or an aborted vehicle launch. The evaluation protocol is based on the needs of 45th Space Wing/Range Safety and 45th Weather Squadron personnel, and designed to provide specific information about the capabilities, limitations, and daily operational use of RAMS in ERDAS at KSC/CCAFS.

The prognostic data from RAMS is available to ERDAS for display and input to the Hybrid Particle and Concentration Transport (HYPACT) model. The HYPACT dispersion model provides three-dimensional dispersion predictions using RAMS forecast grids. Thus, the accuracy of the HYPACT dispersion model is dependent upon the prognostic data from the RAMS model under various weather regimes. This paper briefly discusses the operational RAMS configuration in Section 2, describes the weather regime classification methodology in Section 3, presents a portion of the objective regime classification results in Sections 4 and 5, and provides a summary in Section 6.

2. RAMS CONFIGURATION

In the ERDAS configuration, the three-dimensional, non-hydrostatic mode of RAMS is run operationally on four nested grids with horizontal grid spacing of 60, 15, 5, and 1.25 km, respectively (Fig. 1). The lateral boundary conditions are nudged (Davies 1983) by 12–36-h forecasts from the National Centers for Environmental Prediction 32-km Eta model that have been interpolated onto an 80-km grid. Output from the Eta model is available every 6 h for boundary conditions to RAMS. Two-way interactive boundary conditions are utilized on the inner three grids. The physical parameterization schemes used in RAMS include a cloud microphysics scheme following Cotton *et al.* (1982), a modified Kuo cumulus convection scheme (Tremback 1990), the Chen and Cotton (1988) radiation scheme, a Mellor and Yamada (1982) type turbulence closure, and an 11-layer soil-vegetation model with fixed soil moisture as the initial condition (Tremback and Kessler 1985). The modified Kuo scheme is run on grids 1–3 whereas the 1.25-km grid 4 utilizes explicit convection. The mixed-phase cloud microphysics scheme is run on all four grids.

RAMS is initialized twice-daily at 0000 and 1200 UTC using the Eta 12-h forecast grids and operationally-available observational data including the CCAFS rawinsonde, Aviation Routine Weather Reports, buoys, KSC/CCAFS wind-towers, and KSC/CCAFS 915-MHz and 50-MHz Doppler radar wind profiler data. No variational data assimilation or nudging technique is applied when incorporating observational data. Instead, RAMS is initialized from a cold start by integrating the model forward in time from a gridded field without any balancing or data assimilation steps. For the initial condition, observational data are analyzed onto hybrid coordinates using the RAMS isentropic analysis package (Tremback 1990). Refer to Case *et al.* (2000) for more details on the RAMS hardware and performance characteristics.

RAMS forecast output is available once per hour for display and analysis purposes. Thus, all portions of this model verification study are limited in time to a frequency of one hour, regardless of the frequency of available observational data. This frequency of model output presents a limiting factor in the verification since warm-season weather phenomena in Florida can develop over time scales much shorter than one hour (particularly convection). Nonetheless, hourly forecast output at high spatial resolution has the potential to provide valuable guidance for short-term forecasting in east-central Florida.

3. EVALUATION METHODOLOGY

The complete AMU verification of RAMS consists of an objective and subjective evaluation conducted for a portion of the 1999 Florida warm season (May to August), the 1999-2000 cool season (November to March), and the 2000 warm season (May to September). The objective evaluation consists of point error statistics for all three seasons at several observation locations (grid-4 observation locations shown in Fig. 2), and point error statistics under various meteorological regimes for the 2000 warm-season. The subjective evaluation consists of a verification of the onset and propagation of the East Coast Sea Breeze (ECSB) for the 1999 and 2000 warm-seasons, and precipitation and thunderstorm initiation verifications for the 2000 warm-season months (see Case *et al.* 2001 in this preprint volume). This paper presents the RAMS objective error statistics associated with specific observed surface wind and thunderstorm-day regimes as measured within the KSC/CCAFS wind-tower network. The weather regime classification is used to measure objectively

**Corresponding author address*: Jonathan Case, ENSCO, Inc., 1980 N. Atlantic Ave., Suite 230, Cocoa Beach, FL 32931. Email: case.jonathan@ensco.com

the variations in model accuracy under different meteorological conditions.

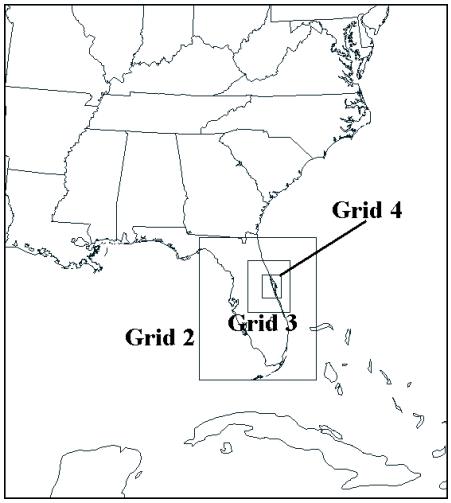

Figure 1. The real-time RAMS domains for the 60-km mesh grid (grid 1) covering much of the southeastern United States and adjacent coastal waters, the 15-km mesh grid (grid 2) covering the Florida peninsula and adjacent coastal waters, the 5-km mesh grid (grid 3) covering east-central Florida and adjacent coastal waters, and the 1.25-km mesh grid (grid 4) covering the area immediately surrounding KSC/CCAFS.

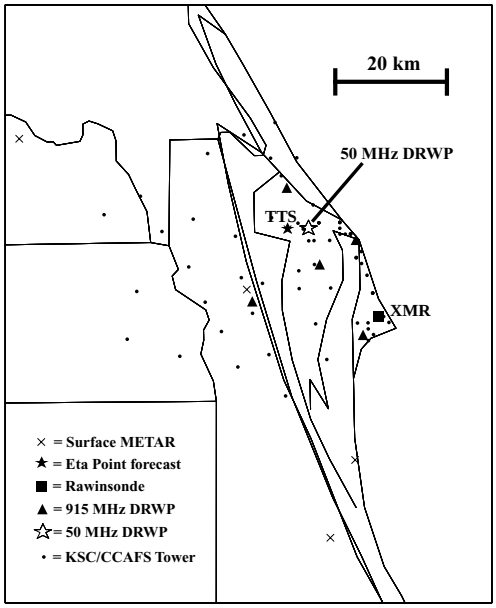

Figure 2. A display of the surface and upper-air stations used for point verification of RAMS forecasts on grid 4. Symbols for the observational data types are given by the key in the lower left of the figure. Only results from the KSC/CCAFS towers and TTS surface station are shown in this paper.

During each day, the surface wind regime was identified according to the early morning wind flow observed within the KSC/CCAFS wind towers of Figure 2. The days were then grouped into three classes of wind-flow patterns: westerly (offshore), easterly (onshore), and light, where light winds were defined as sustained speeds less than 5 knots. The RAMS forecasts were grouped together according to observed surface wind flows (Table 1), and error statistics were compiled for the RAMS forecasts under each surface wind regime. The total number of 1200 UTC forecasts is larger than the 0000 UTC forecasts in Table 1 because the 1200 UTC RAMS cycle contained more successfully completed forecasts during the 2000 warm season. The results of the surface wind regime classification are presented in Section 4.

TABLE 1. The number of RAMS forecasts during the 2000 Florida warm season experiencing early morning surface winds of onshore (easterly component), offshore (westerly component), and light (< 5 knots).

RAMS cycle	Onshore	Offshore	Light
0000 UTC	41	44	32
1200 UTC	46	49	35

For the thunderstorm regime classification, the occurrence of both observed and forecast thunderstorms were recorded for each day of the 2000 warm season. Observed thunderstorm days were identified by the occurrence of cloud-to-ground lightning on grid 4 at any time from 1500–2300 UTC. RAMS forecast thunderstorm days were identified according to the empirical technique described in Case *et al*. (2001). Every day was categorized according to the occurrence of observed and forecast thunderstorms within the area of the grid 4. Each RAMS forecast fell into one of four categories as shown in the contingency table for the 1200 UTC forecast cycle (Table 2). Subsequently, the RAMS point forecast errors at the KSC/CCAFS wind towers were computed during all 24 forecast hours for each of the four possible combinations of observed versus forecast thunderstorm days. The results of the thunderstorm-day regime classification experiment are presented in Section 5.

TABLE 2. A contingency table of the daily occurrence of 1200 UTC RAMS predicted versus observed thunderstorms on grid 4 for all successful forecasts during the 2000 Florida warm season.

1200 UTC Forecast Cycle	Observed T-storms	No Observed T-storms
Forecast T-storms	72	25
No Forecast T-storms	11	38

The point forecast error statistics calculated under the surface wind and thunderstorm-day regimes include the Root Mean Square (RMS) error, bias, and error Standard Deviation (SD) for temperatures and winds. By applying the Murphy (1988) decomposition for RMS error, the SD of the errors were estimated by

$$\mathrm{SD} = \sqrt{\mathrm{RMS}^2 - \mathrm{Bias}^2}\,. \qquad (1)$$

RMS errors can be considered the total error or total difference between the RAMS forecasts and observations, the bias represents the systematic error, and the error SD is the non-systematic or random component of the error. In addition to error quantities, the average values of temperature

forecasts and observations were computed as a function of forecast hour under each weather regime.

4. SURFACE WIND REGIME ERRORS

The 1200 UTC forecast cycle temperature errors under each surface wind regime are shown in Figure 3. The westerly flow regime tends to yield higher predicted daytime temperatures in RAMS as evident by the mean temperature plots in Figure 3a. Among the three surface wind regimes, the light wind regime experiences the largest RMS error (not shown) and cold bias during the afternoon and evening hours (6-12 h in Fig. 3b). The easterly and light wind regimes have a nearly identical pattern of random errors given by the SD in Figure 3c; however, the random portion of the westerly wind regime errors are substantially larger than the other two wind regimes during the late afternoon and evening hours. It is interesting to note that the smallest daytime bias occurs with the westerly wind regime as well.

This relatively larger random error during westerly surface winds is likely the result of an increased occurrence of convection in the vicinity of KSC/CCAFS under this flow regime. Depending on the strength, westerly low-level flow maintains the ECSB boundary in the vicinity of KSC/CCAFS, providing a focusing mechanism for afternoon and evening convection (López and Holle 1987). This convection can subsequently produce significant outflow boundaries resulting in localized temperature gradients and large random errors between the RAMS predicted and observed wind-tower temperatures.

The results of the wind-regime classification also reveal two very apparent characteristics of the wind-direction errors. First, the westerly wind regime contains the largest RMS error during the afternoon and evening hours, likely associated with the higher frequency of convection under low-level westerly flow (Fig. 4). Second, the light wind regime is the primary contributor to the relatively large RMS errors during the late night and early morning hours, as anticipated. Under surface westerly wind flow, the 1200 UTC wind-direction RMS errors reach a maximum of 70–80° between 9–11 h (2100–2300 UTC, Fig. 4). Meanwhile, the RMS errors associated with easterly wind flows are quite small. In fact, during most of the afternoon and evening hours, the RMS error under easterly flow is under 30° (Fig. 4). The daytime RMS errors in light wind regimes are between that of westerly and easterly wind flows.

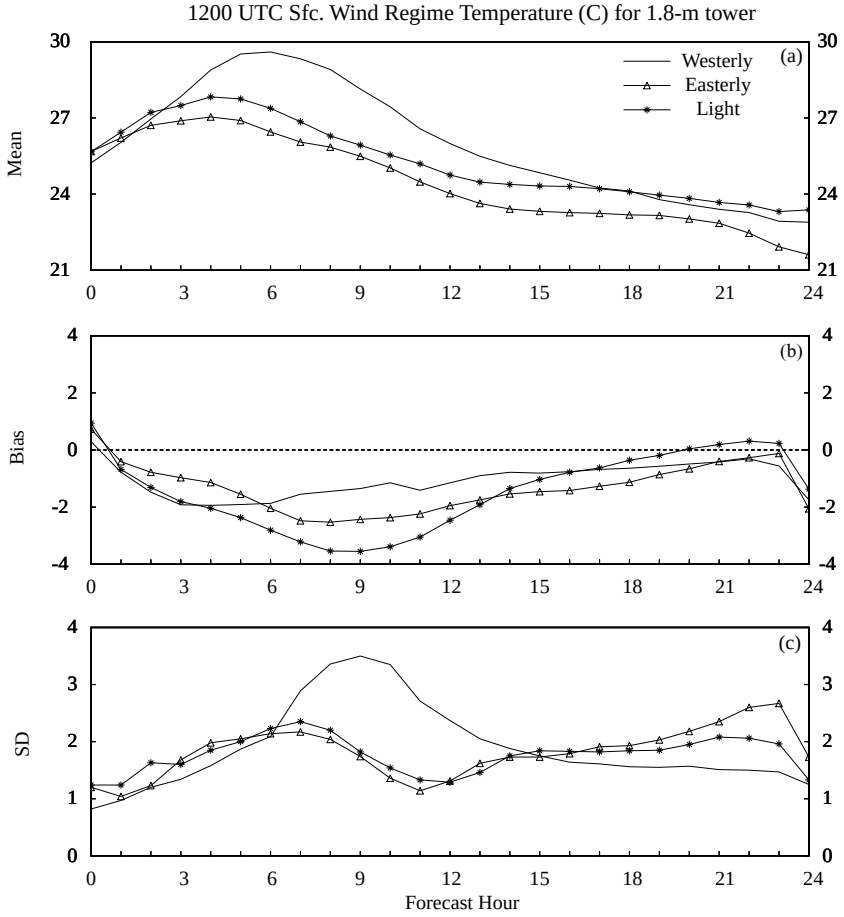

Figure 3. A plot of the 1200 UTC RAMS temperature errors (°C) during westerly (solid line), easterly (triangle), and light surface wind regimes (asterisk) for the 2000 Florida warm season. The temperature is verified at the 1.8-m level of the KSC/CCAFS wind-tower network. Parameters plotted as a function of forecast hour are a) mean forecast temperature under each wind regime, b) bias, and c) error standard deviation (SD).

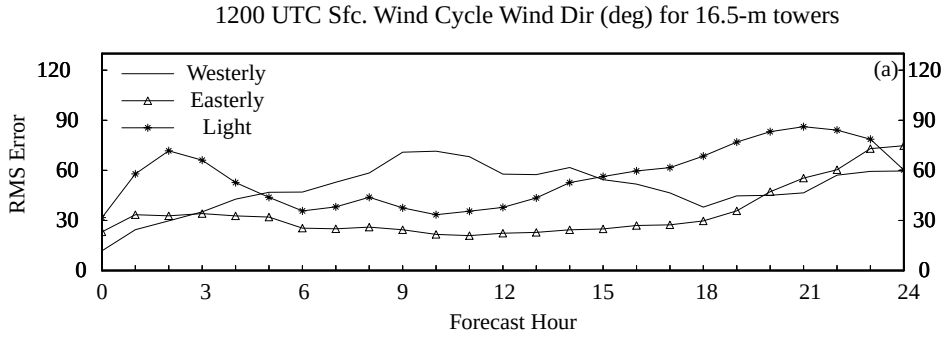

Figure 4. A plot of the 1200 UTC RAMS wind-direction RMS errors (deg.) during westerly (solid line), easterly (triangle), and light surface wind regimes (asterisk) for the 2000 Florida warm season. The wind direction is verified at the 16.5-m level of the KSC/CCAFS wind-tower network.

The largest 1200 UTC wind-direction RMS errors are associated with the light winds that occur between 0–3 h and 18–24 h (Fig. 4). The RMS error grows substantially from 30–70° in the first two forecast hours of the light wind regime (Fig. 4) before tapering as mean wind speeds increase markedly during the day (not shown). The maximum RMS error under light winds occurs during the late night hours (90° at 21 h, or 0900 UTC). These results illustrate how the variable nature of light winds leads to very large errors in wind direction. The wind-direction errors must be used with caution though, because as wind speeds approach zero the wind direction becomes an increasingly meaningless quantity. In these instances, an examination of the individual wind component errors is more appropriate to determine the representative magnitude of the wind errors.

5. THUNDERSTORM REGIME ERRORS

The most significant characteristic of the temperature errors associated with different forecast and observed thunderstorm-day regimes is that the random errors (SD, Fig. 5) are largest during the afternoon and evening hours when thunderstorms are observed. In general, the SD is quite uniform when thunderstorms were not observed (Yes-No and No-No plots in Fig. 5), ranging from 1–2°C for all forecast hours. However, the random forecast errors are markedly larger between 6–12 h during the days when thunderstorms were observed between 1500–2300 UTC (Yes-Yes and No-Yes plots in Fig. 5). These results indicate that observed thunderstorms and associated outflow boundaries appear to have the greatest impact on the random component of the forecast temperature errors in the 1200 UTC cycle, regardless of whether RAMS correctly predicted thunderstorms. The total error (RMS) and bias do not exhibit such a pattern of errors (not shown).

A distinct segregation of errors for observed versus no observed thunderstorm days is also evident in the wind-direction RMS error field for the 1200 UTC forecast cycle, as shown in Figure 6. During the afternoon and evening hours (6–12 h), the wind-direction RMS error increases dramatically when thunderstorms were observed (Yes-Yes and No-Yes plots in Fig. 6). Meanwhile, the RMS error decreases during the same forecast hours on days when thunderstorms were not observed (Yes-No and No-No plots of Fig. 6). These results suggest that the primary contributor to large RMS errors during the afternoon and evening hours is observed thunderstorms, regardless of whether RAMS predicted any thunderstorms.

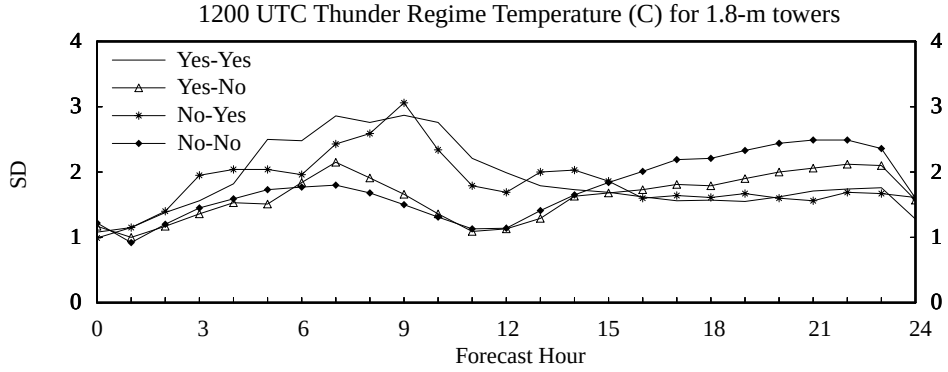

Figure 5. A plot of 1200 UTC RAMS temperature error standard deviation (SD, °C) during the four contingency combinations of thunderstorm forecasts (yes-yes, yes-no, no-yes, no-no) for the 2000 Florida warm season. The temperatures are verified at the 1.8-m level of the KSC/CCAFS wind-tower network.

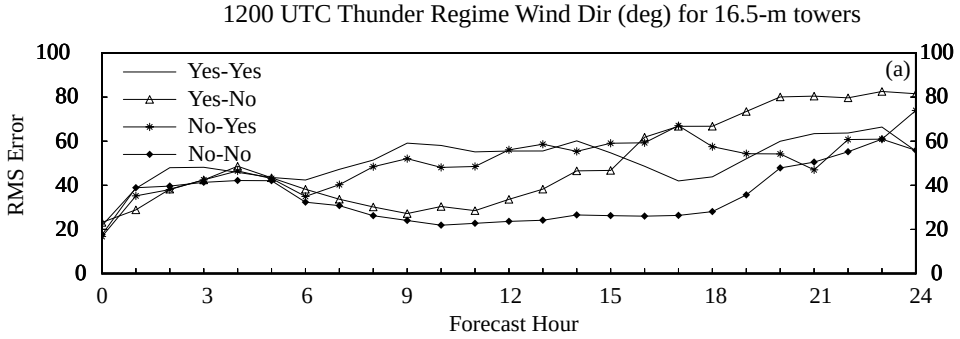

Figure 6. A plot of the 1200 UTC RAMS wind-direction RMS errors (deg.) for the four contingency combinations of thunderstorm forecasts (yes-yes, yes-no, no-yes, no-no) during the 2000 Florida warm season. The wind direction is verified at the 16.5-m level of the KSC/CCAFS wind-tower network.

6. SUMMARY

This paper presented objective model verification results of RAMS as run operationally within ERDAS, according to surface wind and thunderstorm-day weather regimes during the Florida warm-season months of May–September 2000. The meteorological regime classification was used to measure objectively the variations in model accuracy under different weather conditions common to east-central Florida.

Errors in surface point forecasts at the KSC/CCAFS wind towers were computed for three different surface wind regimes: onshore, offshore, and light. In addition, all days during the 2000 Florida warm season were grouped into a 2-by-2 contingency table according to the occurrence of observed versus forecast thunderstorms during the peak convective hours. A RAMS predicted thunderstorm was determined empirically based on a technique described in the companion paper of this preprint volume (Case *et al.* 2001). Surface point forecast errors were calculated for each of the four combinations of observed versus forecast thunderstorm days.

Based on the results presented in this paper, RAMS showed the greatest random errors in forecast surface temperature (~3–4°C) during the afternoon and evening hours under offshore (westerly) surface wind flow and during days with observed thunderstorms. Forecast surface temperature errors did not appear to depend on the accuracy of the RAMS predicted thunderstorm days.

The largest forecast wind-direction RMS errors (approaching 90°) were found under light surface wind regimes during the nocturnal and early morning hours. A secondary maximum in wind-direction RMS errors (~75°) occurred during the afternoon and evening hours associated with offshore surface wind flow. In addition, wind-direction RMS errors diverged after 6 h (1800 UTC) according to the occurrence of observed thunderstorm days. Forecast wind-direction errors increased after 6 h when thunderstorms were observed, and decreased when thunderstorms were not observed. For a copy of the final report on the entire RAMS evaluation as run operationally in ERDAS, please contact the corresponding author listed in this paper.

7. REFERENCES

Case, J. L., J. Manobianco, A. V. Dianic, D. E. Harms, and P. N. Rosati, 2000: A sensitivity and benchmark study of RAMS in the Eastern Range Dispersion Assessment System. Preprints, *9th Conf. on Aviation, Range, and Aerospace Meteorology*, 11-15 September 2000, Orlando, FL, Amer. Meteor. Soc., 426-431.

_____, ____, ____, ____, and ____, 2001: Verification of RAMS forecast sea breezes and thunderstorm initiation over east-central Florida. Preprints, *18th Conf. on Weather Analysis and Forecasting and the 14th Conf. on Numerical Weather Prediction, this volume*.

Chen, S., and W. R. Cotton, 1988: The sensitivity of a simulated extratropical mesoscale convective system to longwave radiation and ice-phase microphysics. *J. Atmos. Sci.*, **45**, 3897-3910.

Cotton, W. R., M. A. Stephens, T. Nehrkorn, and G. J. Tripoli, 1982: The Colorado State University three-dimensional cloud/mesoscale model — 1982. Part II: An ice phase parameterization. *J. de Rech. Atmos.*, **16**, 295-320.

Davies, H. C., 1983: Limitations of some common lateral boundary schemes used in regional NWP models. *Mon. Wea. Rev.*, **111**, 1002-1012.

López, R. E., and R. L. Holle, 1987: Distribution of summertime lightning as a function of low-level wind flow in central Florida. Technical Memorandum, NOAA Environmental Research Labs, Boulder, CO, 43 p.

Mellor, G. L., and T. Yamada, 1982: Development of a turbulence closure model for geophysical fluid problems. *Rev. Geophys. Space Phys.*, **20**, 851-875.

Murphy, A. H., 1988: Skill scores based on the mean square error and their relationships to the correlation coefficient. *Mon. Wea. Rev.*, **116**, 2417-2424.

Tremback, C. J., 1990: Numerical simulation of a mesoscale convective complex: model development and numerical results. Ph.D. Dissertation, Atmos. Sci. Paper No. 465, Department of Atmospheric Science, Colorado State University, Fort Collins, CO 80523, 247 pp.

Tremback, C. J., and R. Kessler, 1985: A surface temperature and moisture parameterization for use in mesoscale numerical models. Preprints, *7th AMS Conf. on Numerical Weather Prediction*, June 17-20, Montreal, Quebec, Amer. Meteor. Soc., Boston, MA, 355-358.